arXiv:1203.2387v3 [hep-ph] 18 May 2013

March 2012

Mirror dark matter interpretations of the DAMA, CoGeNT and CRESST-II data

R. Foot[1]

ARC Centre of Excellence for Particle Physics at the Terascale,
School of Physics, University of Melbourne,
Victoria 3010 Australia

The CRESST-II collaboration have announced evidence for the direct detection of dark matter in 730 kg-days exposure of a $CaWO_4$ target. We examine these new results, along with DAMA and CoGeNT data, in the context of the mirror dark matter framework. We show that all three experiments can be simultaneously explained via kinetic mixing induced elastic scattering of a mirror metal component off target nuclei. This metal component can be as heavy as Fe′ if the galactic rotational velocity is relatively low: $v_{rot} \lesssim 220$ km/s. This explanation is consistent with the constraints from the other experiments, such as CDMS/Ge, CDMS/Si and XENON100 when modest $\sim 20 - 30\%$ uncertainties in energy scale are considered.

[1]E-mail address: rfoot@unimelb.edu.au

1 Introduction

Over the last decade or so, progress has been made in efforts to directly detect dark matter. In particular, the DAMA/NaI [1] and DAMA/Libra [2] experiments have obtained very exciting results in their dark matter search. Recall that these experiments have observed a modulation in the 'single hit' event rate with a period and phase consistent with expectations from dark matter interactions[3]. Background rates are expected to be time independent with the possible exception of muon induced backgrounds. However it has been known for a long time that muons cannot mimic the dark matter annual modulation signature[4]. The DAMA experiments thus provide very convincing evidence that dark matter interactions have been detected.

Another interesting development is the results obtained in the CoGeNT experiment[5]. That experiment features a Germanium target and very low energy threshold. The CoGeNT team observed a rising event rate at low energies. These events could not be explained by known backgrounds and can be interpreted as evidence supporting the DAMA signal. Very recently, the CRESST-II collaboration have announced results for their dark matter search with 730 kg-days of net exposure in a $CaWO_4$ target[6]. The CRESST-II data also cannot be explained by known backgrounds and are compatible with a dark matter signal also rising at low energies.

Attempts to explain the positive signals of DAMA, CoGeNT and CRESST-II in terms of standard WIMP dark matter have proven challenging[7]. However, it has been known for some time[8, 9, 10], that mirror dark matter has a number of novel and distinctive features which make it a suitable candidate to explain the data. In particular mirror dark matter features a mass dependent velocity dispersion $v_0 \propto \frac{1}{\sqrt{m_{A'}}}$, E_R dependent Rutherford scattering $\frac{d\sigma}{dE_R} \propto \frac{1}{E_R^2}$, and particles necessarily in the relevant low mass range. With these features the DAMA and CoGeNT data can be simultaneously explained[11, 12]. The main purpose of this paper is to examine the implications of the new CRESST-II results for mirror dark matter. In the process we will update the CoGeNT analysis taking into account their recently reported surface event correction factor[13]. It turns out that these developments point to new parameter regions within the mirror dark matter framework. Heavy mirror elements, $\sim$ Fe$'$, can explain all three experiments if the galactic rotational velocity is low $v_{rot} \lesssim 220$ km/s. Other regions of parameter space are possible. We explore a few examples in some detail and examine the question of their compatibility with constraints from sensitive but high threshold experiments such as XENON100 and CDMS/Ge.

2 Mirror dark matter and its direct detection

Mirror dark matter posits that the inferred dark matter in the Universe arises from a hidden sector which is an exact copy of the standard model sector[14] (for a review and more complete list of references see ref.[15])[2]. That is, a spectrum of dark matter particles of known masses are predicted: e$'$, H$'$, He$'$, O$'$, Fe$'$,... (with $m_{e'} = m_e$, $m_{H'} = m_H$,

[2]Note that successful big bang nucleosynthesis and successful large scale structure requires effectively asymmetric initial conditions in the early Universe, $T' \ll T$ and $n_{b'}/n_b \approx 5$. See ref.[16] for further discussions.

etc). Kinetic mixing of the $U(1)_Y$ and its mirror counterpart allows ordinary and mirror particles to interact with each other[17]. This $U(1)_Y$ kinetic mixing induces photon-mirror photon kinetic mixing:

$$\mathcal{L}_{mix} = \frac{\epsilon}{2} F^{\mu\nu} F'_{\mu\nu} \tag{1}$$

where $F_{\mu\nu}$ is field strength tensor for the photon and $F'_{\mu\nu}$ is the field strength tensor for the mirror photon. This interaction enables charged mirror sector particles of charge e to couple to ordinary photons with electric charge ϵe [18]. The cross-section of such a particle, say a mirror nucleus, A', with atomic number Z' and velocity v to elastically scatter off an ordinary nucleus (presumed at rest with mass and atomic numbers A, Z) is given by[8]:[3]

$$\frac{d\sigma}{dE_R} = \frac{\lambda}{E_R^2 v^2} \tag{2}$$

where

$$\lambda \equiv \frac{2\pi\epsilon^2 Z'^2 Z^2 \alpha^2}{m_A} F_A^2(qr_A) F_{A'}^2(qr_{A'}) \tag{3}$$

and $F_A(qr_A)$ $[F_{A'}(qr_{A'})]$ is the form factor which takes into account the finite size of the nucleus [mirror nucleus]. A simple analytic expression for the form factor, which we adopt in our numerical work, is the one proposed by Helm[19, 20].

What about the distribution of mirror particles in the galactic halo? These are assumed to be, predominately,[4] roughly spherically distributed in a multi-component plasma containing e$'$, H$'$, He$'$, O$'$, Fe$'$,...[23]. The interaction length is typically much less than a parsec[24] and the dark matter particles form a pressure-supported halo, ideally described by a common temperature, T [5]. This temperature can be estimated from the condition of hydrostatic equilibrium which implies:

$$T = \frac{1}{2} \bar{m} v_{rot}^2 \tag{4}$$

where v_{rot} is the galactic rotational velocity and $\bar{m} = \sum n_{A'} m_{A'} / \sum n_{A'}$ is the mean mass of the particles in the halo. The halo distribution of mirror species is then $f_{A'} = exp(-E/T) = exp(-\frac{1}{2} m_{A'} v^2/T) = exp(-v^2/v_0^2)$. Evidently

$$\begin{aligned} v_0[A'] &= \sqrt{\frac{2T}{m_{A'}}} \\ &= v_{rot} \sqrt{\frac{\bar{m}}{m_{A'}}} \ . \end{aligned} \tag{5}$$

[3]Unless otherwise indicated, we employ natural units where $\hbar = c = 1$.

[4]There may also be a remnant disk of dark mirror stars[21], but constraints from gravitational microlensing (MACHOs searches) limit this component to be subdominant[22].

[5]There are limits on self interactions of dark matter from observations of the Bullet cluster[25]. This sets stringent limits on self interactions provided that the bulk of the dark matter particles are distributed throughout the cluster and not bound to individual galaxies. However mirror dark matter is dissipative and in clusters (or at least in some of them) the bulk of the dark matter particles might be confined in galactic halos [c.f. ref.[26]]. Under this assumption mirror dark matter is consistent with Bullet cluster observations.

The parameter $\bar{m}$ can be estimated within the mirror dark matter model. For a H$'$, He$'$ mass dominated halo, taking into account that the plasma is expected to be fully ionized, we have

$$\frac{\bar{m}}{m_p} \simeq \frac{1}{2 - \frac{5}{4}\xi_{He'}} \tag{6}$$

where $\xi_{He'}$ is the mass fraction of He$'$. The primordial He$'$ abundance can be computed as a function of the kinetic mixing parameter, ϵ, and for $\epsilon \sim 10^{-9}$ the calculations suggest that the primordial He' mass fraction, Y'_p, is around 0.9[27]. If $\xi_{He'} \approx Y'_p$ then Eq.(6) suggests that $\bar{m} \approx 1.1$ GeV. Even if mirror stellar evolution depleted H$'$ further (or somehow depleted both H$'$ and He$'$), this would have only a relatively minor affect on the estimation of $\bar{m}$.

A key feature of this model is that the heavy components with $m_{A'} \gg \bar{m}$ have $v_0[A'] \ll v_{rot}$. This can drastically reduce the tail of the distribution [c.f. standard WIMPs which have $v_0 = v_{rot}$]. This feature can help explain why higher threshold experiments such as CDMS/Ge and XENON100 currently do not see a signal while the lower threshold DAMA and CoGeNT experiments do.

The differential scattering rate for A' elastic scattering on a target nuclei, A, is given by[6]:

$$\frac{dR}{dE_R} = N_T n_{A'} \int_{|\mathbf{v}|>v_{min}}^{\infty} \frac{d\sigma}{dE_R} \frac{f_{A'}(\mathbf{v}, \mathbf{v}_E)}{k} |\mathbf{v}| d^3v \tag{7}$$

where the integration limit, v_{min}, is given by the kinematic relation:

$$v_{min} = \sqrt{\frac{(m_A + m_{A'})^2 E_R}{2 m_A m_{A'}^2}} \, . \tag{8}$$

In Eq.(7), N_T is the number of target nuclei per kg of detector and $n_{A'}$ is the number density of halo dark matter particles, A', at the Earth's location. This number density can be expressed in terms of the halo mass fraction of species A' , $\xi_{A'}$, and total mass density, ρ_{dm} via $n_{A'} = \rho_{dm}\xi_{A'}/m_{A'}$ (we fix $\rho_{dm} = 0.3$ GeV/cm^3). Also in Eq.(7) $\mathbf{v}$ is the velocity of the halo particles relative to the Earth and $\mathbf{v}_E$ is the velocity of the Earth relative to the galactic halo[7]. The halo distribution function, in the reference frame of the Earth, is then given by the Maxwellian distribution:

$$\frac{f_{A'}(\mathbf{v}, \mathbf{v}_E)}{k} = (\pi v_0^2[A'])^{-3/2} exp\left(\frac{-(\mathbf{v} + \mathbf{v}_E)^2}{v_0^2[A']}\right) \, . \tag{9}$$

The integral, Eq.(7), can easily be evaluated in terms of error functions[10, 20] and numerically solved.

[6]The upper limit of integration in Eq.(7) is taken as infinity since we are dealing with dark matter particles with significant self interactions. The self interactions will prevent particles in the high velocity tail of the Maxwellian distribution from escaping the galaxy.

[7]In all numerical work we include an estimate of the Sun's peculiar velocity so that $\langle v_E \rangle = v_{rot} + 12$ km/s.

Bin / keV	Total events	Estimated background
10.2 – 13.0	9	3.2
13 – 16	15	6.1
16 – 19	11	7.0
19 – 25	12	11.5
25 – 40	20	20.1

Table 1: CRESST-II data: total number of events and estimated background.

To compare with the measured event rate, we must include detector resolution effects and overall detection efficiency, $\epsilon_f(E_R^m)$, when the latter is not already included in the experimental results:

$$\frac{dR}{dE_R^m} = \epsilon_f(E_R^m)\frac{1}{\sqrt{2\pi}\sigma_{res}}\int \frac{dR}{dE_R} e^{-(E_R - E_R^m)^2/2\sigma_{res}^2} dE_R \tag{10}$$

where E_R^m is the measured energy and σ_{res} describes the resolution. The measured energy is typically in keVee units (ionization/scintillation energy). For nuclear recoils in the absence of any channeling, keVee = keV/q, where $q < 1$ is the relevant quenching factor. Channeled events, where scattered target atoms travel down crystal axis and planes, have $q \simeq 1$. In light of recent theoretical studies[28], we assume that the channeling fraction is negligible. Channeling, though, is a complicated subject and the modeling used in ref.[28] might miss important physics. Therefore it is, of course, still possible that channeling could play an important role, which could modify the favored regions of parameter space somewhat.

3 Mirror dark matter interpretation of CRESST-II, DAMA/Libra and CoGeNT signals

The CRESST-II experiment

The CRESST-II data[6] arises from 8 detector modules, with recoil energy thresholds (keV) of $10.2, 12.1, 12.3, 12.9, 15.0, 15.5, 16.2, 19.0$. The data is plotted in figure 1. With a view to performing a standard χ^2 analysis of this data, we bin this data into 5 bins, summarized in table 1. This table also indicates the expected background rate estimated from all known sources of background[6].

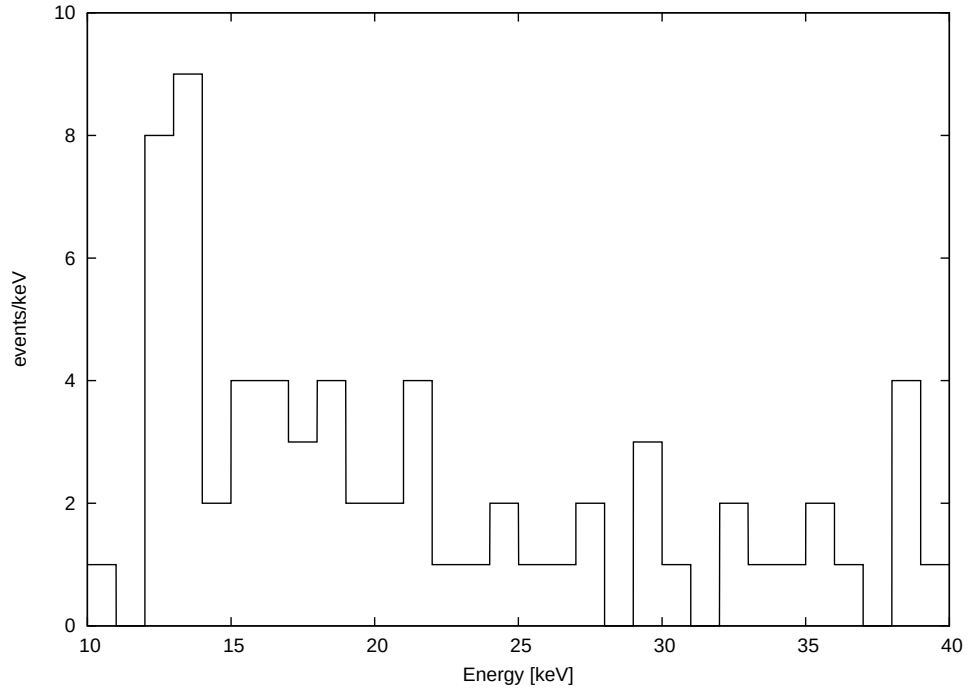


Figure 1: CRESST-II data.

The rates, R_i, relevant for the CRESST-II experiment are computed using Eq.(7) and Eq.(10). As discussed earlier, the halo distributions in Eq.(7) depend on the parameter $\bar{m}$ which has been estimated to be $\bar{m} \approx 1.1$ GeV. A reasonable uncertainty in $\bar{m}$ is $\pm 20\%$, but such a variation does not significantly affect any of our conclusions. We therefore fix $\bar{m} = 1.1$ GeV in all of our numerical work. We use $\sigma_{res} = 0.3$ keV[6] and assume detection efficiencies for the three target elements: $\epsilon_f = 0.90$ for O, W and $\epsilon_f = 1.0$ for Ca, which take into account their acceptance region. As per previous analysis[11, 12] we make the simplifying assumption that the mirror metal components are dominated by a single element A' in a given experiment. This can only be an approximation, however it can often be a reasonable one given the relatively narrow energy range probed in the experiments [e.g. the signal region in the experiments are mainly: 2-4 keVee (DAMA), 0.5-1 keVee (CoGeNT), 12-14 keV (CRESST-II)]. With this assumption and assuming a particular value for v_{rot}, the fit to the data depends on two parameters $m_{A'}$, $\epsilon\sqrt{\xi_{A'}}$. [8] We define χ^2 for the CRESST-II data in the usual way:

$$\chi^2(m_{A'}, \epsilon\sqrt{\xi_{A'}}) = \sum_{i=1}^{5} \left[\frac{R_i + B_i - data_i}{\delta data_i} \right]^2 \tag{11}$$

where R_i is the theoretically predicted rate and B_i is the estimated background in the i^{th} energy bin. We evaluate χ^2 as per Eq.(11), with the constraint $m_{A'} \leq m_{Fe} \simeq 55.8 m_p$. We have not considered any uncertainty in the CRESST-II energy scale.

[8] In our numerical work we allow A', Z' to have non-integer values, with $Z' = A'/2$ (except when we specifically consider $A' = \mathrm{Fe}'$, then $Z' = 26$ and $A' \simeq 56$). Since the realistic case involves a spectrum of elements, the effective mass number can be non-integer.

The DAMA annual modulation signal

For DAMA we analyse the annual modulation signal using the 12 bins of width 0.5 keVee in the energy range: $2-8$ keVee[2] taking into account the detector resolution[29]. An important issue is the nuclear recoil energy scale which is set by the values of the quenching factors $q_{Na},\ q_I$. In the recent analysis[11, 12] we used $q_{Na} = 0.30 \pm 0.06$, $q_I = 0.09 \pm 0.02$, where the central values were taken from averages over a large range of energies[1]. However quenching factors are in general energy dependent and many measurements of q_I tend to show increasing values in the important low energy region. This is also supported by some theoretical arguments based on the classical Birks forumula[30]. [See e.g. ref.[31] for a summary figure of much of the available information]. In view of the current situation, we allow for a range of possible values for the quenching factors:

$$q_{Na} = 0.28 \pm 0.08, \quad q_I = 0.12 \pm 0.08 \tag{12}$$

We minimize χ^2 varying $q_{Na},\ q_I$ over the above range of values (assumed energy independent for simplicity). Values of $q_I,\ q_{Na}$ outside the above range are certainly possible, such as the higher values $q_{Na} \approx 0.6,\ q_I \approx 0.3$ suggested by Tretyak[30]. While we don't specifically consider the possibility of such high quenching factors in the numerical work presented here, qualitatively we note that higher quenching factors generally move the DAMA allowed region to lower values of $\epsilon\sqrt{\xi_{A'}},\ m_{A'}$ and also yields interesting parameter space overlapping with that from CoGeNT and CRESST-II.

The CoGeNT experiment

Our analysis procedure for CoGeNT is different to our earlier analysis[11, 12]. It has been pointed out that there may be surface events contaminating CoGeNT's signal region[13] which have not been excluded by CoGeNT's rise time cut. Preliminary estimates indicate that this can be a very large effect - the signal may be reduced by a factor of around 0.3 in the important low energy region ($E_R < 1.0$ keVee)[13, 32]. In view of this we analyse CoGeNT data using 15 bins of width 0.1 keVee in the region $0.5 - 2.0$ keVee. We take the efficiency corrected and surface event corrected CoGeNT data from figure 4 of ref.[32]. We allow a constant background, which we fit to the data in this energy range. We have taken into account some uncertainties in energy scale by minimizing the χ^2 for CoGeNT over the variation in quenching factor, $q_{Ge} = 0.21 \pm 0.04$. Obviously, the CoGeNT spectrum is quite uncertain at the present time and one could easily assign $\sim 40\%$ uncertainty in the rate. Such an uncertainty would imply a $\sim 20\%$ uncertainty in inferred values of $\epsilon\sqrt{\xi_{A'}}$ from CoGeNT data. This is in addition to the uncertainties we have considered. Thus, the reader should be aware that the favored region we derive for CoGeNT might move considerably as future data is accumulated and the backgrounds are better understood.

The analysis

Table 2 gives the χ^2_{min} values obtained from the fit to the DAMA annual modulation and CoGeNT, CRESST-II spectrum data for a fixed value of $v_{rot} = 200$ km/s, which we have found as an example where all three experiments have overlapping favored regions of parameter space. The value $v_{rot} = 200$ km/s is around 20% less than some recent estimates of this quantity[33]. However allowing for a small bulk halo rotation, e.g. in a

Experiment	$\chi^2(min)/d.o.f.$	Best fit parameters
DAMA (annual mod.)	5.7/10	$\frac{m_{A'}}{m_p} = 55.8$, $\epsilon\sqrt{\xi_{A'}}/10^{-10} = 2.5$
CoGeNT (spectrum)	15.7/12	$\frac{m_{A'}}{m_p} = 42.0$, $\epsilon\sqrt{\xi_{A'}}/10^{-10} = 1.7$
CRESST (spectrum)	2.6/3	$\frac{m_{A'}}{m_p} = 55.8$, $\epsilon\sqrt{\xi_{A'}}/10^{-10} = 2.7$

Table 2: Summary of $\chi^2(min)$ for the relevant data sets from the DAMA, CoGeNT and CRESST-II experiments. [Here $v_{rot} = 200$ km/s].

co-rotating halo, a $10\% - 20\%$ smaller *effective* v_{rot} value can easily be envisaged. There are also significant astrophysical uncertainties in this quantity.

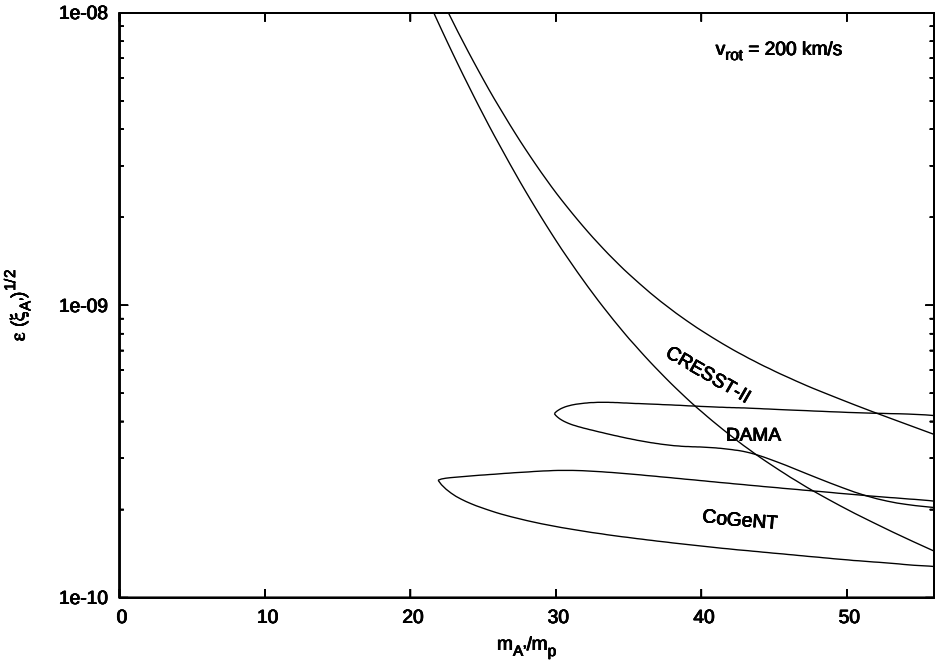


Figure 2: DAMA, CoGeNT and CRESST-II favored regions of parameter space in the mirror dark matter model for $v_{rot} = 200$ km/s.

The 90% (99%) C.L. favored region of parameter space is bounded by the contours where $\chi^2(m_{A'}, \epsilon\sqrt{\xi_{A'}}) = \chi^2_{min} + 4.6(9.2)$. In figure 2 we plot the CRESST-II 90% C.L. favored region along with the 99% C.L. favored region of parameter space for DAMA

Experiment	$\chi^2(min)/d.o.f.$	Best fit parameters
DAMA (annual mod.)	5.5/10	$v_{rot} = 210$ km/s , $\epsilon\sqrt{\xi_{A'}}/10^{-10} = 3.1$
CoGeNT (spectrum)	15.8/12	$v_{rot} = 201$ km/s , $\epsilon\sqrt{\xi_{A'}}/10^{-10} = 1.6$
CRESST (spectrum)	0.3/3	$v_{rot} = 250$ km/s , $\epsilon\sqrt{\xi_{A'}}/10^{-10} = 1.7$

Table 3: Summary of $\chi^2(min)$ for the relevant data sets from the DAMA, CoGeNT and CRESST-II experiments for $A' = \mathrm{Fe}'$.

and CoGeNT[9].

Figure 2 indicates that in the high mass region, $m_{A'} \gtrsim 50 m_p$ including $A' \sim \mathrm{Fe}'$, DAMA encompasses lower $\epsilon\sqrt{\xi_{A'}}$ values. This is because dark matter scattering on Iodine becomes kinematically favored and can dominate over Sodium scattering in this parameter region. The resulting lower values of $\epsilon\sqrt{\xi_{A'}}$ produce a favored region of parameter space overlapping with that of the other experiments. If the spectrum of mirror dark matter elements has some resemblance to ordinary matter, we might expect Fe' to be the dominant heavy mirror metal component. To study this possibility further we fix $A' = \mathrm{Fe}'$ ($m_{A'} = 55.8 m_p$) and vary v_{rot} in the range: $160 \leq v_{rot}(\mathrm{km/s}) \leq 250$. The resulting χ^2_{min} values are given in table 3. Expanding around these χ^2_{min} values we obtain the CRESST-II 90% C.L. and the DAMA, CoGeNT 99% C.L. favored parameter regions in figure 3.

[9]The CoGeNT experiment does not discriminate electron recoils from nuclear recoils. In principle, e' inelastic scattering on bound electrons in the target can therefore also contribute to the signal at low energies $E_R \lesssim$ keVee. Previous work[34, 11] has indicated that the e' contribution can be comparable to the rate of nuclear recoils. However, the previous analysis[34, 11] assumed that the flux of e' at the detector was much larger than the flux of mirror nuclei due to the large dispersion velocity $v_0[e'] \gg v_{rot}$. In reality this cannot be the case. A larger flux of e' would lead to a greater rate of e' capture in the Earth c.f. mirror nuclei capture, and hence this would lead to an increasing mirror electric charge within the Earth, Q'_E. In fact, we expect Q'_E to be generated such that the flux of e' and mirror nuclei at the Earth's surface approximately equalize. Taking this effect into account reduces the expected e' flux by more than an order of magnitude, leaving nuclear recoils as the dominant contribution to the rate.

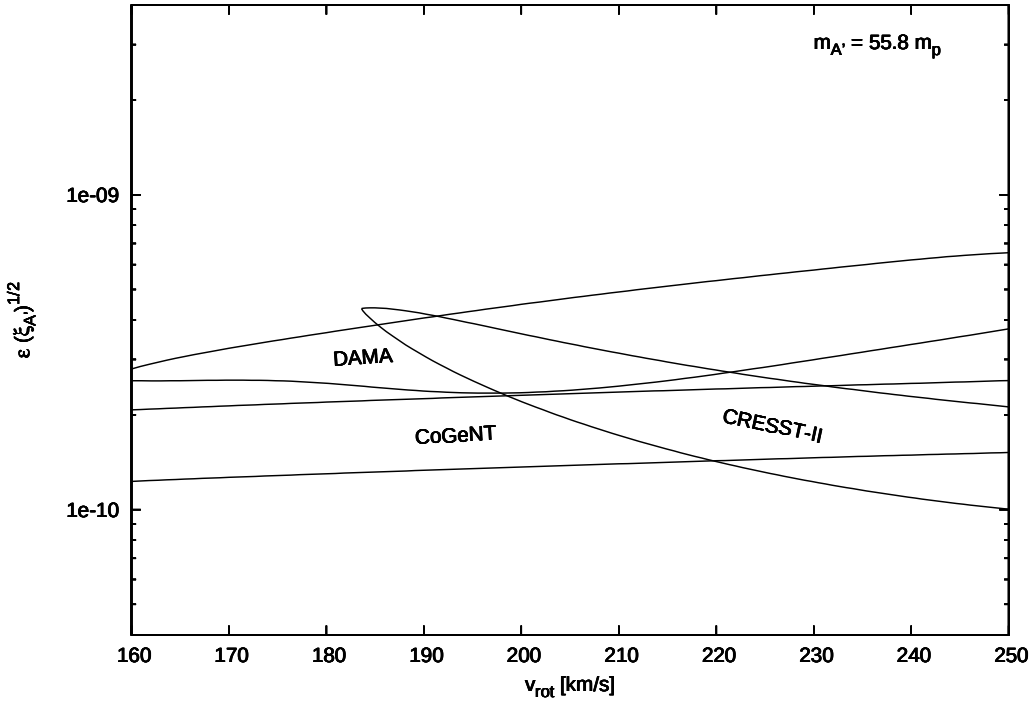


Figure 3: DAMA, CoGeNT and CRESST-II favored regions of parameter space in the mirror dark matter model for $A' = \mathrm{Fe}'$ (i.e. $m_{A'} = 55.8 m_p$).

4 Two examples, P1 and P2

As discussed earlier, the systematic uncertainties are potentially quite significant for CoGeNT. The favored region can move up or down by $\sim 20\%$ as future data is collected and backgrounds are better understood. A small channeling fraction or quenching factors outside the range considered in Eq.(12), can also move the DAMA region somewhat. In this light, figures 2,3 offer some encouragement as they indicate some parameter space where all three experiments can be explained by Fe' scattering. At this point one could combine all three of these experiments and do a fit using the combined χ^2. However, in view of the potentially large systematic uncertainties it is not clear how useful such a combined analysis would be. Instead we consider two example reference points. The first one is located near the overlapping allowed regions indicated in figure 2:

$$P1 : A' \;=\; \mathrm{Fe}' \; (m_{Fe'} \simeq 55.8 m_p), \; v_{rot} = 200 \text{ km/s}, \; \epsilon\sqrt{\xi_{Fe'}} = 2.2 \times 10^{-10} \; . \quad (13)$$

Figure 4a,b,c, compares the predicted rates assuming the $P1$ parameter set with the relevant DAMA, CoGeNT and CRESST-II data.

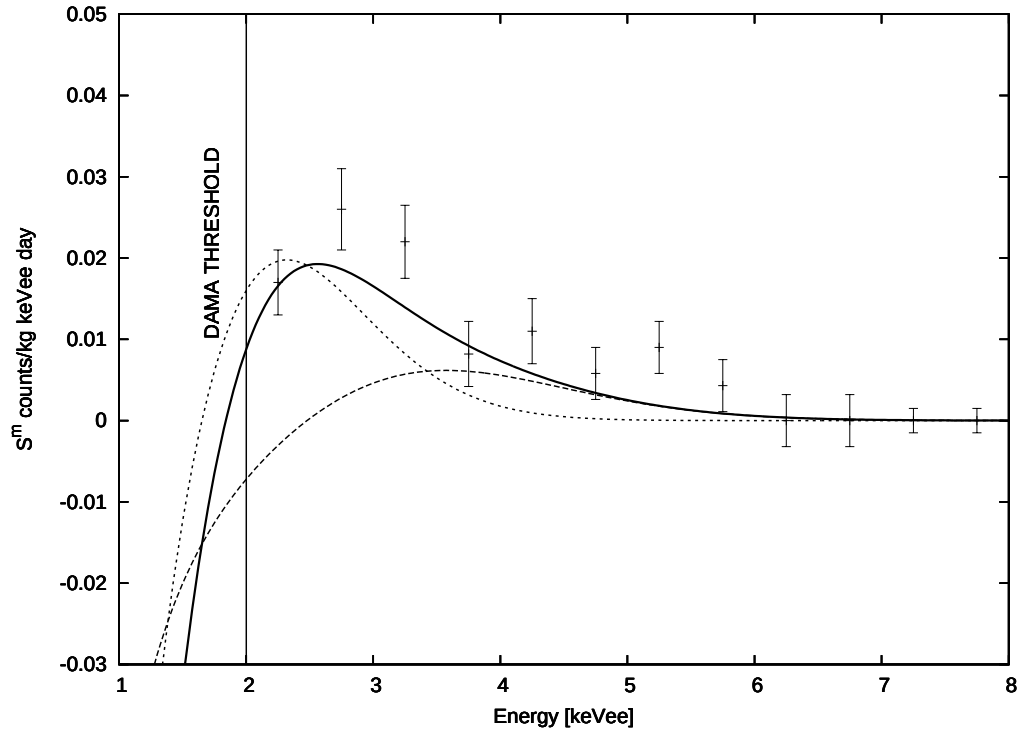


Figure 4a: DAMA annual modulation spectrum for mirror dark matter with parameter choice $P1$ (solid line). The separate contributions from dark matter scattering off Sodium (dashed line) and Iodine (dotted line) are shown. In this example $q_{Na} = 0.33,\ q_I = 0.20$.

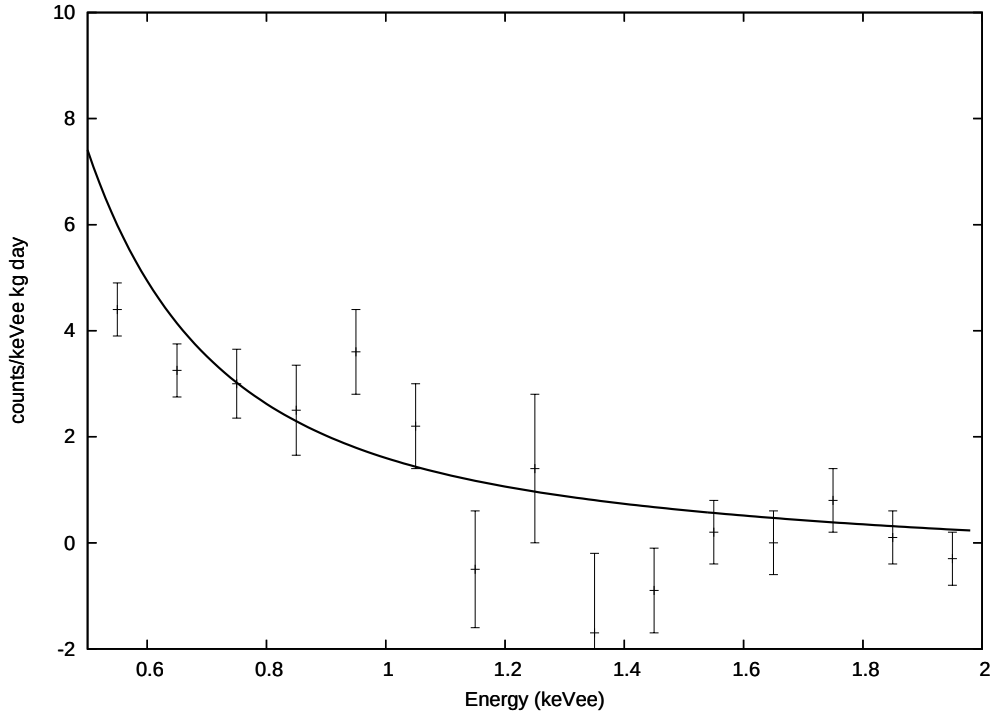


Figure 4b: CoGeNT spectrum for mirror dark matter with parameters $P1$ (solid line). In this example $q_{Ge} = 0.17$.

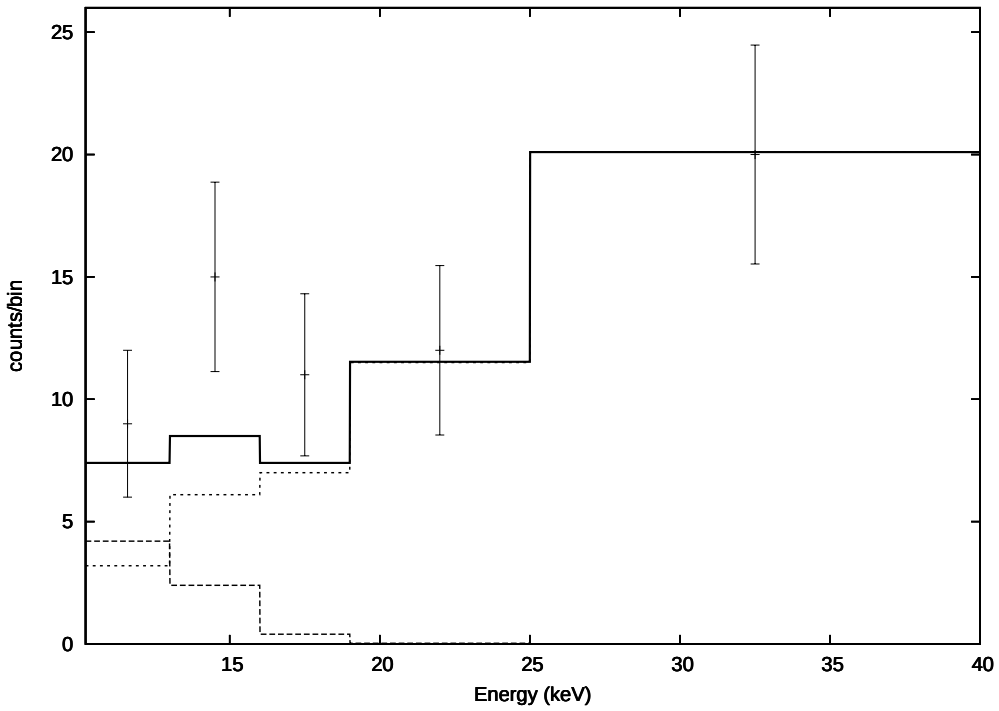


Figure 4c: CRESST-II spectrum for mirror dark matter with parameters $P1$ (solid line). The signal component (dashed line) and background component (dotted line) are also shown.

For the example point $P1$, the CRESST-II signal is dominated by Fe$'$ scattering on the Ca target element. Of course the reasons for this are purely kinematical being due to $m_{Fe'} \sim m_{Ca}$.

The change in sign of the annual modulation amplitude at low energies indicated in figure 4a will not necessarily hold if there are lighter more abundant components such as O$'$, Ne$'$. The positive contributions to the annual modulation amplitude from these lighter components can overwhelm the negative contribution due to the heavier components at low energies. We illustrate this point with the following example:

$$P2 : A' = \mathrm{Fe}',\ \epsilon\sqrt{\xi_{Fe'}} = 1.7 \times 10^{-10},\ \xi_{O'}/\xi_{Fe'} = 10,\ v_{rot} = 210 \text{ km/s} . \qquad (14)$$

Figure 5a,b,c, compares the predicted rates for the reference point $P2$ with the relevant DAMA, CoGeNT and CRESST-II data.

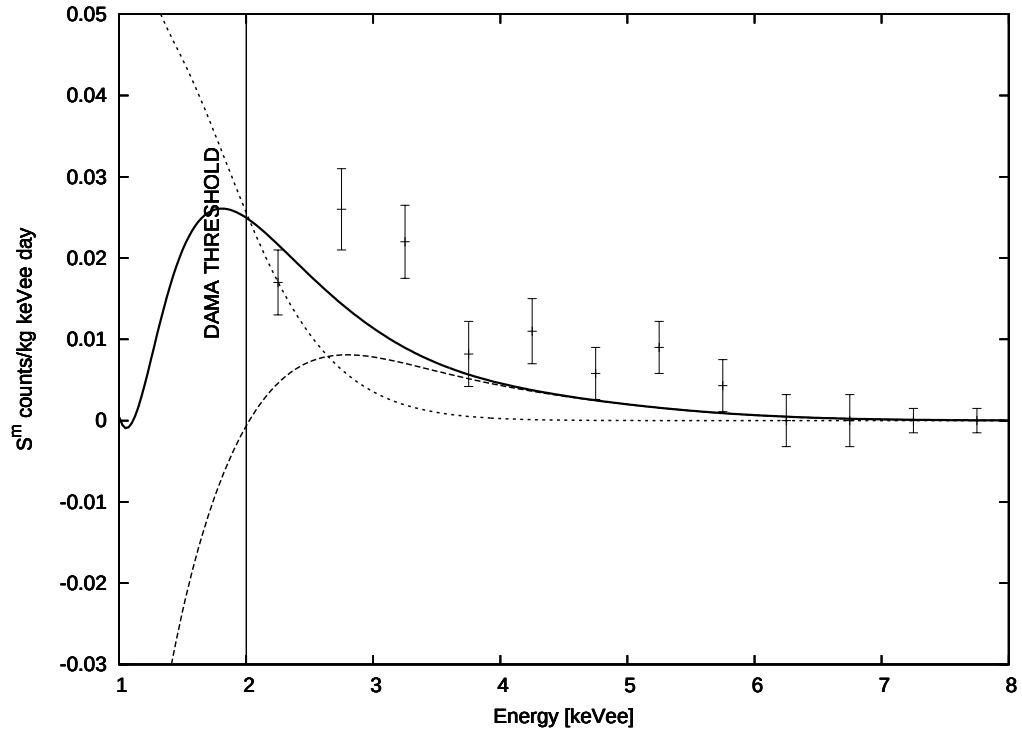


Figure 5a: DAMA annual modulation spectrum for mirror dark matter with parameters $P2$ (solid line). The separate contributions from Fe$'$ interactions (dashed line) and O$'$ (dotted line) interactions are also shown. In this example $q_{Na} = 0.34$, $q_I = 0.20$.

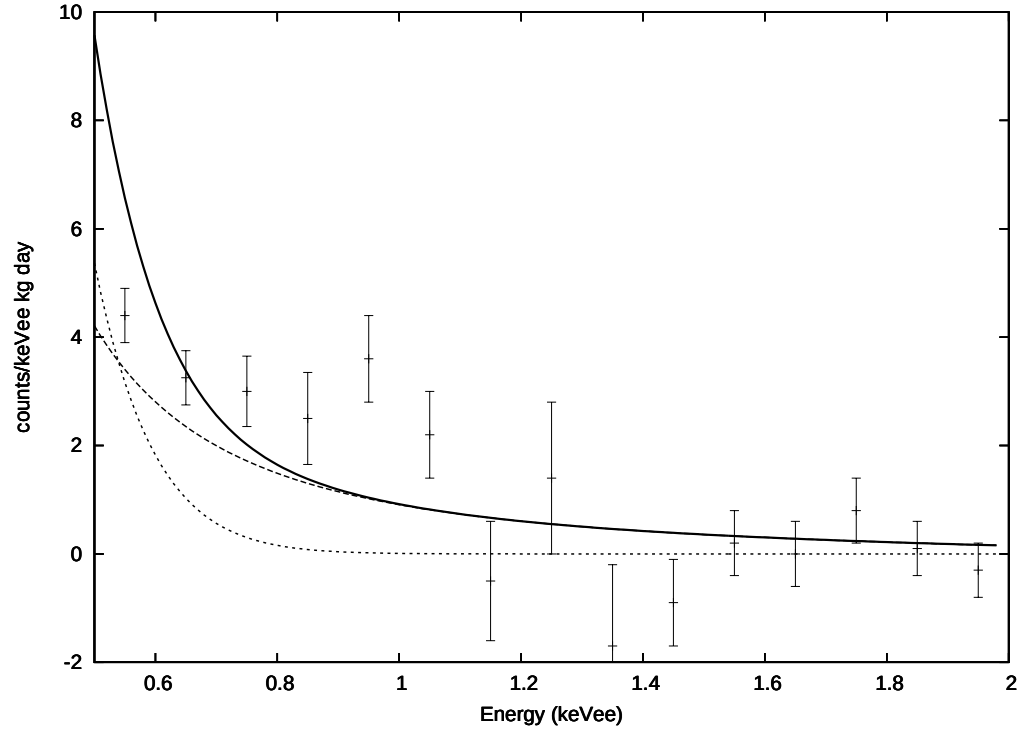


Figure 5b: CoGeNT spectrum for mirror dark matter with parameters $P2$ (solid line). The separate contributions from Fe$'$ interactions (dashed line) and O$'$ (dotted line) interactions are

also shown. In this example $q_{Ge} = 0.17$.

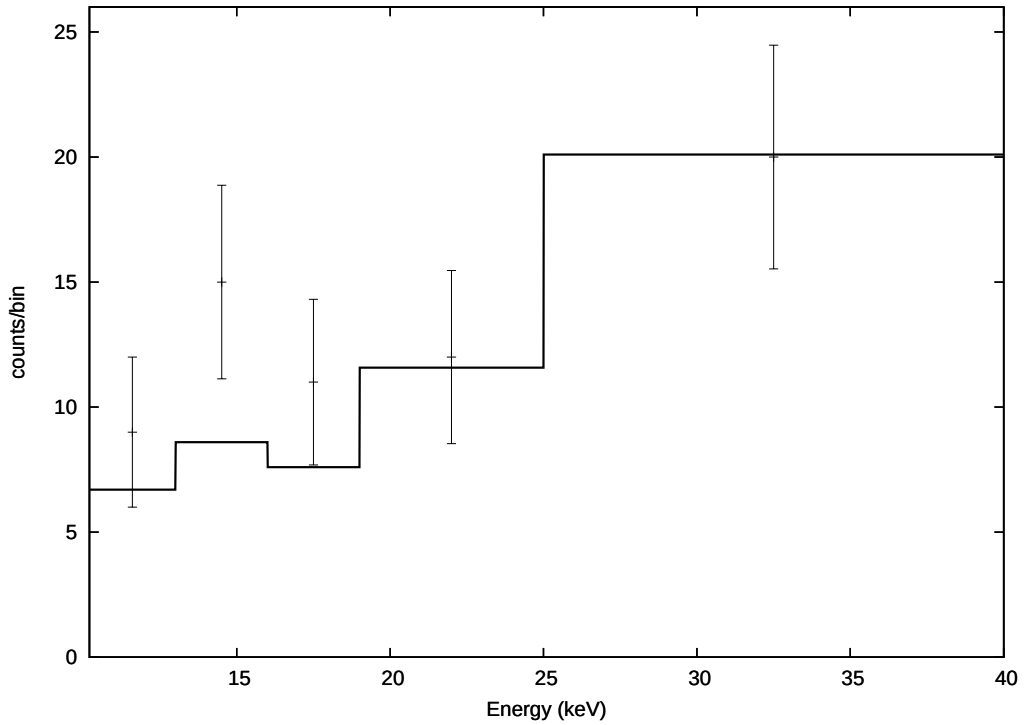


Figure 5c: CRESST-II spectrum for mirror dark matter with parameters $P2$ (solid line).

Figures 5 show that with low $v_{rot} \lesssim 220$ km/s light metal components ($\sim$ O$'$) and lighter components (H$'$, He$'$) can be kinematically suppressed in DAMA, CoGeNT and CRESST-II. Future experiments at lower thresholds, such as Texono[35], should be able to probe such light components.

Observe that the dark matter signal contribution in CRESST-II is relatively low in these examples. However it could easily be enhanced in many ways. Increasing $\epsilon\sqrt{\xi_{A'}}$ will increase the rate in CRESST-II and improve the fit in DAMA and is therefore an obvious possibility. Another possibility is that the CRESST-II energy scale might be overestimated by e.g. $\sim 10\%$. If CRESST-II events are at lower energies then this can increase the expected rate in CRESST-II. Also, a slight increase in $\bar{m}$ of order $\sim 20\%$ can greatly improve the fit in CRESST-II. Such small changes of $\bar{m}$ do not significantly affect DAMA or CoGeNT since these experiments are sensitive to dark matter in the body of the Maxwellian distribution[11] while CRESST-II is probing interactions in the tail of the dark matter velocity distribution (in this example).

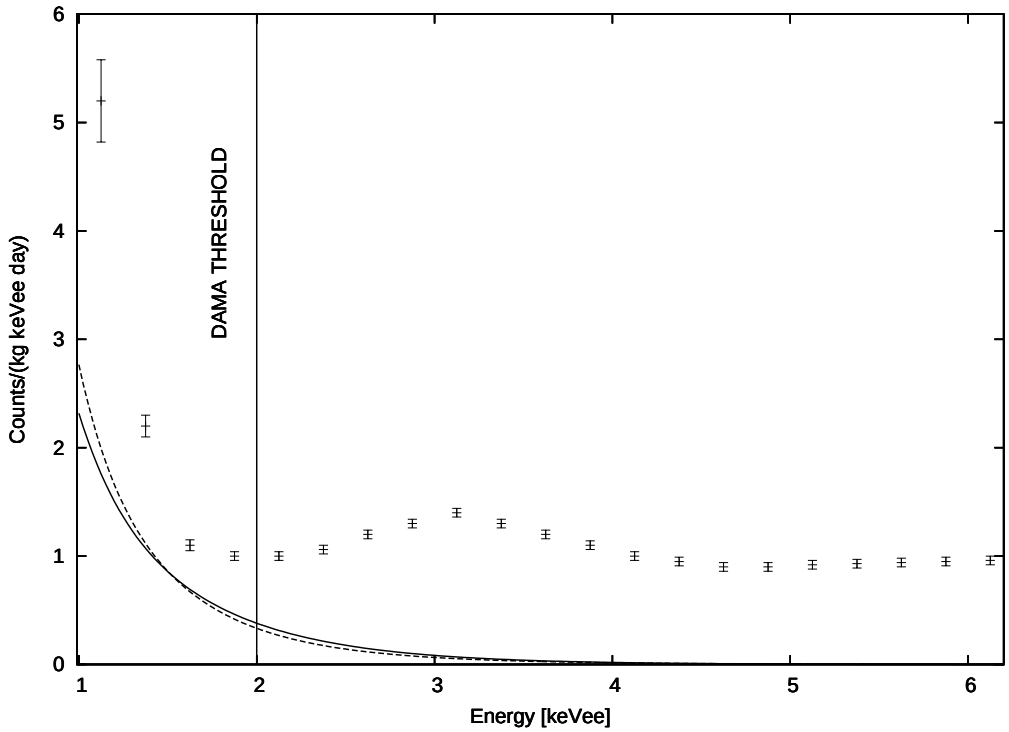


Figure 6: DAMA spectrum for mirror dark matter with parameters $P1$ (solid line), $P2$ (dashed line). In this example $q_{Na} = 0.34$, $q_I = 0.20$.

Future data from DAMA, CoGeNT, CRESST-II and other experiments will obviously be able to constrain the parameter space within the mirror dark matter framework. As discussed recently[36], a particularly striking diurnal modulation signal should be observable for a detector located in the southern hemisphere, and maybe even in a detector in the northern hemisphere at low latitudes, such as detectors in Jin-Ping Underground laboratory. In the meantime, we must rely on annual modulation and spectrum data. In figure 6 we give the predicted spectrum for DAMA/Libra and Figure 7 the predicted annual modulation spectrum in CoGeNT for each reference point, $P1$, $P2$ [detection efficiency = 1 for these figures]. Clearly, the initial annual modulation amplitude measured by CoGeNT to be $A \approx 0.46 \pm 0.17$ cpd/kg/keVee averaged over the energy range: $0.5 < E(\text{keVee}) < 3.0$, is much larger than that predicted by our example points. It will be interesting to see if CoGeNT's hint of a large annual modulation amplitude is confirmed by CDEX, C-4, and other experiments.

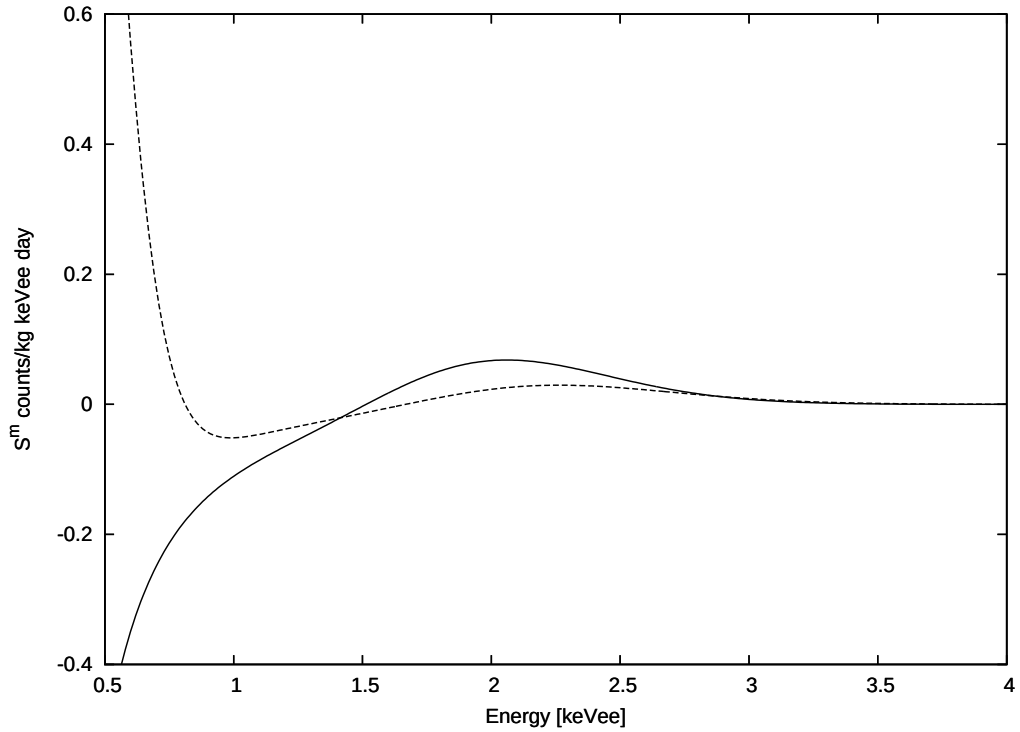


Figure 7: CoGeNT annual modulation spectrum for mirror dark matter with parameters $P1$ (solid line), $P2$ (dashed line). In this example $q_{Ge} = 0.17$.

Let us make a few comments. Firstly, there are alternative explanations of DAMA, CoGeNT and CRESST-II within the mirror dark matter framework. For example, if v_{rot} is high ($\gtrsim$ 240 km/s) then DAMA and CoGeNT can be mainly detecting the lighter metal components $\sim$ O$'$-Si$'$ [11, 12]. In this case, it is possible that CRESST-II might be seeing a less abundant heavier component (e.g. Fe$'$), or even the same component if v_{rot} is very high $\gtrsim$ 260 km/s. Secondly, more generic hidden sector dark matter can also explain the data in a similar way to the mirror dark matter case. One simply requires a hidden sector with two or more stable particles charged under an unbroken $U(1)'$ gauge interaction which is kinetically mixed with standard $U(1)_Y$[12, 10]. These ingredients can arise, for example, in spontaneously broken mirror models[37].

Finally, observe that the experiments constrain $\epsilon\sqrt{\xi_{A'}}$ but do not allow for a precise determination of ϵ or $\xi_{A'}$ separately. It is difficult to estimate $\xi_{A'}$. Mirror metals might be generated in mirror stars, presumably at an early epoch[38]. It might also be possible to produce the metal component in the early Universe, although this is disfavored in the simplest scenarios with high reheating temperature[27]. A third possibility is that the average metal component is actually very low in the galaxy, $\langle\xi_{A'}\rangle \ll 10^{-2}$, but its abundance is greatly enhanced in the galactic disk. One possible mechanism for this is the influence of the galactic magnetic field[39] which can potentially exclude (or suppress) light elements ($m_{A'} \lesssim m_{O'}$) from entering the disk[24] (see also ref.[40]). This could thereby enhance the proportion of heavier components whose abundance should increase until the pressure equalizes with that of the rest of the halo (at the same radial distance). In this case $\xi_{A'} \sim 1$ is possible within the disk, i.e. at the detector's location.

Experiment	95% C.L limit	E_R^{est} threshold	E_R^{nom} threshold	$100\left[1-\frac{E_R^{nom}}{E_R^{est}}\right]$
CDMS/Ge	6.3	13.1 keV	10.0 keV	23.7%
CDMS/Si	3.0	8.5 keV	7.0 keV	17.6 %
XENON100	4.7	12.9 keV	8.4 keV	34.9 %

Table 4: Estimated energy threshold (E_R^{est}) for which the CDMS/Ge, CDMS/Si and XENON100 experiments are consistent with the mirror dark matter expectations assuming the example point, $P1$. E_R^{nom} is the nominal energy threshold of each experiment. The last column gives the percentage at which the energy threshold needs to have been underestimated for the point $P1$ to be consistent with these experiments at 95% C.L.

The above possibilities suggest a broad range for $\xi_{A'}$: $10^{-4} \lesssim \xi_{A'} \lesssim 1$. If the direct detection experiments are due to mirror dark matter with $\epsilon\sqrt{\xi_{A'}} \sim$ few 10^{-10} then this suggests that ϵ is in the range[10] $\sim 10^{-10} - 10^{-8}$. The most stringent laboratory limit on ϵ arises from invisible decays of orthopositronium[43, 44], $\epsilon \lesssim 1.5 \times 10^{-7}$. An important proposal exists[45] for a more sensitive orthopositronium experiment which can cover much of the ϵ range of interest. Also, note that values of $\epsilon \gtrsim 10^{-9}$ can also be probed in early Universe cosmology[46]. In particular, forthcoming results expected from the Planck mission might shed some light on ϵ in the near future. There are also other interesting possible effects of the kinetic mixing[15, 47].

5 Constraints from CDMS and XENON100

Let us now examine the question of the compatibility of this model with the constraints from the XENON100[48], CDMS/Ge[49] and CDMS/Si[50] experiments[11]. This question is somewhat non-trivial since the answer depends sensitively on the recoil energy threshold which (typically) has at least 20% uncertainty and often the subject of controversy. The XENON100 experiment, which has the largest exposure, has especially poor knowledge of energy calibration in the important low energy region (see ref.[54, 55] for relevant discussions). In view of the above, we explore the compatibility question by estimating the energy threshold for which the parameter point $P1$ can be excluded at 95% C.L. [The constraint on $P2$ is similar to that of $P1$]. We have taken into account the relevant detection efficiencies, exposure time etc, although we conservatively ignore effects of detector resolution for the XENON100 experiment. Our results are given in table 4. Note that the 95% C.L. limits in the second column arise since CDMS/Ge, CDMS/Si and XENON100 observed $2, 0, 1$ events respectively in the low energy region.

Table 4 indicates that mirror dark matter with parameters given by the example $P1$ is consistent with the CDMS/Ge, CDMS/Si and XENON100 data provided that the

[10]Similar values of ϵ can be motivated from an astrophysical argument. Mirror dark matter is dissipative and radiative cooling would cause the halo to collapse on a time scale of a few hundred million years unless a substantial heat source exists. Kinetic mixing induced processes in the core of ordinary supernova (such as $e'\bar{e}'$ production via plasmon decay[41]) can supply the energy needed to compensate for the energy lost from the halo due to radiative cooling if $\epsilon \sim 10^{-9}$[23, 42].

[11]There are also lower threshold analysis by the XENON10[51] and CDMS collaborations[52]. However it has been argued[53] that neither analysis can exclude light dark matter when systematic uncertainties are properly taken into account.

energy scale has been underestimated by of order $20-30\%$ respectively. This level of energy scale uncertainty is within critical assessments of these experiments discussed in the literature. We conclude that the considered mirror dark matter explanation of the DAMA, CoGeNT and CRESST-II data is consistent with the data from CDMS/Si, CDMS/Ge and XENON100 experiments when reasonable systematic uncertainties in energy scale are included. It should also be noted that the two events seen in CDMS/Ge and also the events seen just above the threshold in the Edelweiss experiment[56] are both compatible with dark matter interactions within this model given these energy scale uncertainties.

Finally, the KIMS experiment[31] is currently running with a ~ 100 kg CsI target. They have reported a (2σ) limit on the rate of dark matter interactions from a Pulse Shape Analysis (PSA) of their spectrum: $R < 0.02$ cpd/kg/keVee for $3.0 < E_R(\text{keVee}) < 4.0$. We find that the Iodine interaction rate in a CsI target predicted by mirror dark matter for the particular point $P1$ is $R \approx 0.006$ cpd/kg/keVee in the $3 < E_R(\text{keVee}) < 4$ bin and falling sharply at higher energies. [Assuming here that KIMS has the same resolution and q_I quenching factor as the DAMA/Libra experiment]. Thus, their PSA does not constrain mirror dark matter. However, the KIMS experiment also aims to measure/constrain the annual modulation amplitude. The annual modulation results are anticipated to be reported within the coming year. Assuming that they can reach a similar energy threshold to DAMA, they can potentially see a positive signal for a signficant portion of parameter space (c.f dotted line in figure 4a).

6 Conclusion

In conclusion, we have examined the new results from the CRESST-II experiment along with the latest results from DAMA and CoGeNT experiments in the context of the mirror dark matter framework. In this framework dark matter consists of a spectrum of mirror elements: H$'$, He$'$, O$'$, Fe$'$, ... of known masses. Under the simplifying but reasonable assumption that DAMA, CoGeNT and CRESST-II might be observing a particular dark matter component, A', we have found that mirror dark matter models can explain the data from each experiment. In particular, we have found that each experiment can be explained by $A' \sim$ Fe$'$ interactions if $\epsilon\sqrt{\xi_{Fe'}} \approx 2 \times 10^{-10}$ and $v_{rot} \sim 200$ km/s. Other regions of parameter space are possible. We have also shown that the considered explanation is consistent with the results of the other experiments when reasonable systematic uncertainties in energy scale are considered.

Acknowledgments

The author would like to thank Juan Collar, Juhee Lee and Leo Stodolsky for helpful correspondence. This work was supported by the Australian Research Council.

References

[1] R. Bernabei *et al.* (DAMA Collaboration), Riv. Nuovo Cimento. **26**, 1 (2003) [astro-ph/0307403]; Int. J. Mod. Phys. E**13**, 2127 (2004); Phys. Lett. B**480**, 23 (2000).

[2] R. Bernabei *et al.* (DAMA Collaboration), Eur. Phys. J. C**67**, 39 (2010) [arXiv: 1002.1028]; Eur. Phys. J. C**56**, 333 (2008) [arXiv:0804.2741].

[3] A. K. Drukier, K. Freese and D. N. Spergel, Phys. Rev. D**33**, 3495 (1986); K. Freese, J. A. Frieman and A. Gould, Phys. Rev. D**37**, 3388 (1988).

[4] R. Bernabei *et al.*, arXiv:1202.4179.

[5] C. E. Aalseth *et al.* (CoGeNT Collaboration), Phys. Rev. Lett. **106**, 131301 (2011) [arXiv:1002.4703]; Phys. Rev. Lett. **107**, 141301 (2011) [arXiv: 1106.0650].

[6] G. Angloher, M. Bauer, I. Bavykina, A. Bento, C. Bucci, C. Ciemniak, G. Deuter and F. von Feilitzsch *et al.*, arXiv:1109.0702.

[7] C. Savage, G. Gelmini, P. Gondolo and K. Freese, JCAP **0904**, 010 (2009) [arXiv:0808.3607]; C. Savage, G. Gelmini, P. Gondolo and K. Freese, Phys. Rev. D **83**, 055002 (2011) [arXiv:1006.0972]; Y. Mambrini, JCAP **1009**, 022 (2010) [arXiv:1006.3318]; D. Hooper, J. I. Collar, J. Hall, D. McKinsey and C. Kelso, Phys. Rev. D **82**, 123509 (2010) [arXiv:1007.1005]; P. J. Fox, J. Liu and N. Weiner, Phys. Rev. D **83** (2011) 103514 [arXiv:1011.1915]; J. L. Feng, J. Kumar, D. Marfatia and D. Sanford, Phys. Lett. B **703**, 124 (2011) [arXiv:1102.4331]; C. Arina, J. Hamann and Y. Y. Y. Wong, JCAP **1109**, 022 (2011) [arXiv:1105.5121]; D. Hooper and C. Kelso, Phys. Rev. D **84**, 083001 (2011) [arXiv:1106.1066]; P. Belli, R. Bernabei, A. Bottino, F. Cappella, R. Cerulli, N. Fornengo and S. Scopel, Phys. Rev. D **84**, 055014 (2011) [arXiv:1106.4667]; T. Schwetz and J. Zupan, JCAP **1108**, 008 (2011) [arXiv:1106.624]; M. Farina, D. Pappadopulo, A. Strumia and T. Volansky, JCAP **1111**, 010 (2011) [arXiv:1107.0715]; P. J. Fox, J. Kopp, M. Lisanti and N. Weiner, Phys. Rev. D **85**, 036008 (2012) [arXiv:1107.0717]; C. McCabe, Phys. Rev. D **84**, 043525 (2011) [arXiv:1107.0741]; N. Fornengo, P. Panci and M. Regis, Phys. Rev. D **84**, 115002 (2011) [arXiv:1108.4661]; J. M. Cline and A. R. Frey, Phys. Lett. B **706**, 384 (2012) [arXiv:1109.4639]; J. Kopp, T. Schwetz and J. Zupan, arXiv:1110.2721]; M. T. Frandsen, F. Kahlhoefer, C. McCabe, S. Sarkar and K. Schmidt-Hoberg, JCAP **1201**, 024 (2012) [arXiv:1111.0292]; P. Gondolo and G. B. Gelmini, arXiv:1202.6359.

[8] R. Foot, Phys. Rev. D**69**, 036001 (2004) [hep-ph/0308254].

[9] R. Foot, Mod. Phys. Lett. A**19**, 1841 (2004) [astro-ph/0405362]; astro-ph/0403043; Phys. Rev. D**74**, 023514 (2006) [astro-ph/0510705].

[10] R. Foot, Phys. Rev. D**78**, 043529 (2008) [arXiv: 0804.4518].

[11] R. Foot, Phys. Rev. D**82**, 095001 (2010) [arXiv: 1008.0685]; Phys. Lett. B**692**, 65 (2010) [arXiv: 1004.1424].

[12] R. Foot, Phys. Lett. B **703**, 7 (2011) [arXiv:1106.2688].

[13] Talk by J. Collar, TAUP 2011 workshop, Munich, Germany Sep 5-9, 2011.

[14] R. Foot, H. Lew and R. R. Volkas, Phys. Lett. B**272**, 67 (1991); Mod. Phys. Lett. A**7**, 2567 (1992).

[15] R. Foot, Int. J. Mod. Phys. D**13**, 2161 (2004) [astro-ph/0407623]; Int. J. Mod. Phys. A**19** 3807 (2004) [astro-ph/0309330]; P. Ciarcelluti, Int. J. Mod. Phys. D**19**, 2151 (2010) [arXiv: 1102.5530].

[16] H. M. Hodges, Phys. Rev. D**47**, 456 (1993); Z. Berezhiani, D. Comelli and F. L. Villante, Phys. Lett. B**503**, 362 (2001) [hep-ph/0008105]; L. Bento and Z. Berezhiani, Phys. Rev. Lett. **87**, 231304 (2001) [hep-ph/0107281]; A. Yu. Ignatiev and R. R. Volkas, Phys. Rev. D**68**, 023518 (2003) [hep-ph/0304260]; R. Foot and R. R. Volkas, Phys. Rev. D**68**, 021304 (2003) [hep-ph/0304261]; Phys. Rev. D**69**, 123510 (2004) [hep-ph/0402267]; Z. Berezhiani, P. Ciarcelluti, D. Comelli and F. L. Villante, Int. J. Mod. Phys. D**14**, 107 (2005) [astro-ph/0312605]; P. Ciarcelluti, Int. J. Mod. Phys. D**14**, 187 (2005) [astro-ph/0409630]; Int. J. Mod. Phys. D**14**, 223 (2005) [astro-ph/0409633]. For pioneering work, see: S. I. Blinnikov and M. Yu. Khlopov, Sov. J. Nucl. Phys. **36**, 472 (1981); Sov. Astron. **27**, 371 (1983).

[17] R. Foot and X-G. He, Phys. Lett. B**267**, 509 (1991).

[18] B. Holdom, Phys. Lett. B **166**, 196 (1986).

[19] R. H, Helm, Phys. Rev. **104**, 1466 (1956).

[20] J. D. Lewin and P. F. Smith, Astropart. Phys. **6**, 87 (1996).

[21] Z. K. Silagadze, Phys. Atom. Nucl. **60**, 272 (1997) [Yad. Fiz. **60N2**, 336 (1997)] [hep-ph/9503481]; R. Foot, Phys. Lett. B **452**, 83 (1999) [astro-ph/9902065].

[22] C. Alcock *et al.* [MACHO Collaboration], Astrophys. J. **542**, 281 (2000) [astro-ph/0001272]. P. Tisserand *et al.* [EROS-2 Collaboration], Astron. Astrophys. **469**, 387 (2007) [astro-ph/0607207].

[23] R. Foot and R. R. Volkas, Phys. Rev. D**70**, 123508 (2004) [astro-ph/0407522].

[24] R. Foot, Phys. Lett. B**699**, 230 (2011) [arXiv:1011.5078].

[25] D. Clowe, M. Bradac, A. H. Gonzalez, M. Markevitch, S. W. Randall, C. Jones and D. Zaritsky, Astrophys. J. **648**, L109 (2006) [astro-ph/0608407].

[26] Z. K. Silagadze, ICFAI U. J. Phys. **2**, 143 (2009) [arXiv:0808.2595].

[27] P. Ciarcelluti and R. Foot, Phys. Lett. B**690**, 462 (2010) [arXiv:1003.0880].

[28] N. Bozorgnia, G.B. Gelmini and P. Gondolo, JCAP **1011**, 019 (2010) [arXiv: 1006.3110]; JCAP **1011**, 028 (2010) [arXiv: 1008.3676].

[29] R. Bernabei *et al.* [DAMA Collaboration], Nucl. Instrum. Meth. A **592**, 297 (2008) [arXiv:0804.2738].

[30] V. I. Tretyak, Astropart. Phys. **33**, 40 (2010) [arXiv:0911.3041].

[31] S. K. Kim, on behalf of the KIMS collaboration, TAUP 2011 workshop, Munich, Germany Sep 5-9, 2011.

[32] C. Kelso, D. Hooper and M. R. Buckley, Phys. Rev. D **85**, 043515 (2012) [arXiv:1110.5338].

[33] A. Brunthaler, M. J. Reid, K. M. Menten, X. -W. Zheng, A. Bartkiewicz, Y. K. Choi, T. Dame and K. Hachisuka *et al.*, arXiv:1102.5350.

[34] R. Foot, Phys. Rev. D **80**, 091701 (2009) [arXiv:0909.3126].

[35] Q. Yue *et al.* [for the CDEX-TEXONO Collaboration], arXiv:1201.5373.

[36] R. Foot, arXiv:1110.2908.

[37] J. -W. Cui, H. -J. He, L. -C. Lu and F. -R. Yin, arXiv:1110.6893.

[38] Z. Berezhiani, S. Cassisi, P. Ciarcelluti and A. Pietrinferni, Astropart. Phys. **24**, 495 (2006) [astro-ph/0507153].

[39] L. Chuzhoy and E. W. Kolb, JCAP **0907**, 014 (2009) [arXiv:0809.0436].

[40] S. D. McDermott, H. -B. Yu and K. M. Zurek, Phys. Rev. D **83**, 063509 (2011) [arXiv:1011.2907].

[41] G. G. Raffelt, *Chicago, USA: Univ. Pr. (1996) 664 p.*

[42] R. Foot and Z. K. Silagadze, Int. J. Mod. Phys. D **14**, 143 (2005) [astro-ph/0404515].

[43] S. L. Glashow, Phys. Lett. B **167**, 35 (1986); R. Foot and S. N. Gninenko, Phys. Lett. B **480**, 171 (2000) [hep-ph/0003278]; S. V. Demidov, D. S. Gorbunov and A. A. Tokareva, Phys. Rev. D **85**, 015022 (2012) [arXiv:1111.1072].

[44] A. Badertscher, P. Crivelli, W. Fetscher, U. Gendotti, S. Gninenko, V. Postoev, A. Rubbia and V. Samoylenko *et al.*, Phys. Rev. D **75**, 032004 (2007) [hep-ex/0609059].

[45] P. Crivelli, A. Belov, U. Gendotti, S. Gninenko and A. Rubbia, JINST **5**, P08001 (2010) [arXiv:1005.4802].

[46] R. Foot, arXiv:1111.6366; P. Ciarcelluti and R. Foot, Phys. Lett. B **679**, 278 (2009) [arXiv:0809.4438] and references there-in.

[47] R. Foot and S. Mitra, Astropart. Phys. **19**, 739 (2003) [astro-ph/0211067]; Phys. Lett. A**315**, 178 (2003) [cond-mat/0306561]; Phys. Lett. B**558**, 9 (2003) [astro-ph/0301229]; S. Mitra, Phys. Rev. D **74**, 043532 (2006) [astro-ph/0605369].

[48] E. Aprile *et al.* [XENON100 Collaboration], Phys. Rev. Lett. **107**, 131302 (2011) [arXiv:1104.2549].

[49] Z. Ahmed *et al.* [The CDMS-II Collaboration], Science **327**, 1619 (2010) [arXiv:0912.3592].

[50] J. P. Filippini, Ph. D. thesis (2008).

[51] J. Angle *et al.* [XENON10 Collaboration], Phys. Rev. Lett. **107**, 051301 (2011) [arXiv:1104.3088].

[52] Z. Ahmed *et al.* [CDMS-II Collaboration], Phys. Rev. Lett. **106**, 131302 (2011) [arXiv:1011.2482].

[53] J. I. Collar, arXiv:1103.3481 ; arXiv:1106.0653 .

[54] J. I. Collar, arXiv:1010.5187.

[55] R. Cerulli *et al.*, arXiv:1201.4582.

[56] E. Armengaud *et al.* [EDELWEISS Collaboration], Phys. Lett. B **702**, 329 (2011) [arXiv:1103.4070].